



## Synthesis, antiviral activity and molecular modeling of oxoquinoline derivatives

Fernanda da C. Santos<sup>a</sup>, Paula Abreu<sup>b</sup>, Helena C. Castro<sup>b</sup>, Izabel C. P. P. Paixão<sup>b,\*</sup>, Claudio C. Cirne-Santos<sup>d</sup>, Viveca Giongo<sup>b</sup>, Juliana E. Barbosa<sup>b</sup>, Bruno R. Simonetti<sup>b</sup>, Valéria Garrido<sup>b</sup>, Dumith Chequer Bou-Habib<sup>d</sup>, David de O. Silva<sup>a</sup>, Pedro N. Batalha<sup>a</sup>, Jairo R. Temerozo<sup>d</sup>, Thiago M. Souza<sup>b</sup>, Christiane M. Nogueira<sup>a</sup>, Anna C. Cunha<sup>a</sup>, Carlos R. Rodrigues<sup>c</sup>, Vitor F. Ferreira<sup>a</sup>, Maria C. B. V. de Souza<sup>a,\*</sup>

<sup>a</sup> Universidade Federal Fluminense, Instituto de Química, Departamento de Química Orgânica, Programa de Pós-Graduação em Química, Outeiro de São João Batista, s/n, Centro, Niterói, CEP 24210-150, RJ, Brazil

<sup>b</sup> Universidade Federal Fluminense, Instituto de Biologia, Departamento de Biologia Celular e Molecular, Programa de Pós Graduação em Neurociências, Outeiro de São João Batista s/n, Centro, Niterói, CEP 24020-150, RJ, Brazil

<sup>c</sup> Laboratório de Modelagem Molecular e QSAR (ModMolQSAR), Faculdade de Farmácia, Universidade Federal do Rio de Janeiro, Rio de Janeiro, CEP 21941-590, RJ, Brazil

<sup>d</sup> Laboratório de Pesquisas Sobre o Timo, Instituto Oswaldo Cruz/Fiocruz, Rio de Janeiro, RJ 21045-900, Brazil

### ARTICLE INFO

#### Article history:

Received 18 April 2009

Revised 17 June 2009

Accepted 18 June 2009

Available online 24 June 2009

This paper is dedicated to late Professor Octávio Augusto Ceva Antunes to acknowledge his many contributions to organic chemistry

#### Keywords:

Antiviral

HIV-1

Oxoquinoline

Structure–activity relationship (SAR)

### ABSTRACT

In the present article, we describe the synthesis, anti-HIV1 profile and molecular modeling evaluation of 11 oxoquinoline derivatives. The structure–activity relationship analysis revealed some stereoelectronic properties such as LUMO energy, dipole moment, number of rotatable bonds, and of hydrogen bond donors and acceptors correlated with the potency of compounds. We also describe the importance of substituents R<sup>2</sup> and R<sup>3</sup> for their biological activity. Compound **2j** was identified as a lead compound for future investigation due to its : (i) high activity against HIV-1, (ii) low cytotoxicity in PBMC, (iii) low toxic risks based on in silico evaluation, (iv) a good theoretical oral bioavailability according to Lipinski 'rule of five', (v) higher druglikeness and drug-score values than current antivirals AZT and efavirenz.

© 2009 Elsevier Ltd. All rights reserved.

## 1. Introduction

Acquired immunodeficiency syndrome (AIDS) caused by the human immunodeficiency virus (HIV) remains a health threat of global significance. Although the highly active anti-retroviral therapy (HAART) effectively reduced the mortality rate and prolonged the life expectancy in developing and developed countries, it has not eradicated HIV-1 from the infected tissues.<sup>1</sup> The powerful drug cocktails can suppress virus replication, often keeping blood levels so low as to be undetectable by standard tests.<sup>2</sup> Since viral replication remains active in cellular reservoirs, the long-term use of the combined therapy is mandatory but in a restricted way due to the increased prevalence of HIV-1 resistant strains, metabolic disorders, and complex administration.<sup>3</sup> Therefore, the search for new antiretroviral agents is crucial, and compounds that inhibit different steps of HIV-1 replication cycle are under development or clinical investigation. In contrast to the failed attempts at developing a

vaccine against HIV, efforts to provide drug therapies stand as a great success.

Quinolone derivatives are a class of potential drugs that may contribute to the control of the latent HIV-1 reservoir.<sup>4</sup> Oxoquinoline ribonucleoside **1** has been shown to inhibit HIV-1 replication in vitro in both acutely and chronically HIV-infected cell lines by interfering with Tat-mediated transcription.<sup>5</sup>

Due to the need of new antivirals to deal with the HIV-resistance to antivirals, we have been testing the oxoquinoline derivatives against HIV virus replication in order to search for biologically active compounds.<sup>5</sup> We have recently identified chloroquinolinic ribonucleoside 6-chloro-1,4-dihydro-4-oxo-1-(D-ribofuranosyl)-quinoline-3-carboxylic acid (**1**) as an inhibitor of the RNA-dependent DNA polymerase (RDDP) activity of HIV1-Reverse Transcriptase with uncompetitive and noncompetitive modes of action with respect to dTTP incorporation and to template/primer (TP) uptake, respectively. Interestingly, this compound presents an extremely low cytotoxic effect compared to AZT.<sup>6</sup> Nucleoside analogs are prodrugs that require conversion to their triphosphate forms by cellular kinases to target the

\* Corresponding authors. Tel.: +55 21 26292361; fax: +55 21 26292135 (M.C.B.V.S.).  
E-mail address: [gqocica@vm.uff.br](mailto:gqocica@vm.uff.br) (M.C.B.V. de Souza).

transcriptase reverse enzyme, to become active even in uninfected cells. On the contrary, this oxoquinoline derivative (**1**) inhibits HIV-1 replication without requiring any phosphorylation reaction, what may explain its low toxicity. Besides, this compound presented additive effects with AZT and nevirapine and a synergistic effect with the protease inhibitor atazanavir, classical drugs currently used in antiretroviral therapy.<sup>6</sup>

In this work, based on the chloroxoquinolinic ribonucleoside (**1**), we planned a new series of oxoquinoline derivatives (**2a–k**) to identify a structure–activity relationship. Thus, we performed changes in structural and electronic properties as the replacement of the riboside ring by hydrogen (**2a** and **2h–i**) and hydrophobic group such as benzyl (**2b–c**) (subunit A–R<sup>3</sup> position). We also tested the ring-opening of riboside (acyclic chain, **2d–g** and **2j–k**) (R<sup>3</sup> position). We changed the chlorine by the fluorine atom in the R<sup>1</sup> position (**2e**, **2g**, **2k**) in order to increase the electronegativity effect. In addition, we performed the substitution of the acidic function by other different functional groups in the R<sup>2</sup> position (subunit B): ethyl ester (**2a–b**, **2d–e**), hydrazide (**2f–h**) or amide (**2i–k**) (Scheme 1).

## 2. Results and discussion

### 2.1. Chemistry

Compounds **2a–c** and **2h** (Scheme 2) were prepared by standard procedures.<sup>7–10</sup> We have previously described acyclonucleosides **2d** and **2e**.<sup>11</sup>

Carboxamides **2i** and **2i'** (Scheme 2) were prepared by nucleophilic substitution at the carbonyl ester using benzylamine as the nucleophile and phenyl ether as the solvent, at 210 °C.<sup>9</sup> Then, previous silylation of these oxoquinolines by heating with bis(trimethylsilyl)trifluoroacetamide (BSTFA)<sup>11</sup> containing 1% of trimethylchlorosilane (TMCS), in acetonitrile, under reflux, followed by addition of equimolar amount of 1,3-dioxolane, chlorotrimethylsilane, and potassium iodide, at room temperature, and subsequent neutralization with solid sodium bicarbonate afforded the new acyclonucleosides **2j** and **2k** (Scheme 2).

Acyclonucleosides **2d** and **2e** (Scheme 2) were submitted to nucleophilic substitution reaction with hydrazine monohydrate (80%)<sup>9</sup> in refluxing ethanol affording acylhydrazides **2f** and **2g** in good yields, 75 and 70%, respectively.

### 2.2. Biological assays

#### 2.2.1. Anti-HIV-1 effect

The oxoquinolines were also evaluated for their inhibitory effect on HIV virus replication. The EC<sub>50</sub> values were calculated by comparing p24 antigen concentrations in supernatants of treated infected cells with those in supernatants of untreated infected cells at day 7 postinfection. Significant dose-dependent antiviral

activities were observed for compounds **2f** (EC<sub>50</sub> = 2.5 μM), **2g** (EC<sub>50</sub> = 3.3 μM), **2j** (EC<sub>50</sub> = 4.5 μM), and **2k** (EC<sub>50</sub> = 2.8 μM).

#### 2.2.2. Cytotoxicity effect

The evaluation of oxoquinoline derivatives using results of peripheral blood mononuclear cells (PBMCs) showed that none of the compounds were cytotoxic (Table 1). The CC<sub>50</sub> values revealed that compounds **2f** (CC<sub>50</sub> = 2400 μM), **2j** (CC<sub>50</sub> = 3200 μM), and **2k** (CC<sub>50</sub> = 2800 μM) were less cytotoxic than other compounds and also better than AZT (CC<sub>50</sub> = 126 μM) and **1** (CC<sub>50</sub> = 1701 μM) under the same assay conditions.<sup>6</sup> This reflects the low cytotoxicity of these compounds, which is in agreement with their high selective index (SI) (Table 1). The SI calculated based on the ratio of CC<sub>50</sub> and EC<sub>50</sub> showed **2f**, **2j**, and **2k** with the best results (960, 711, and 1000, respectively). In fact, they were close to AZT (SI = 2520) and better than the commercial antivirals DDC (SI = 110) and DDI (SI = 10).<sup>12</sup>

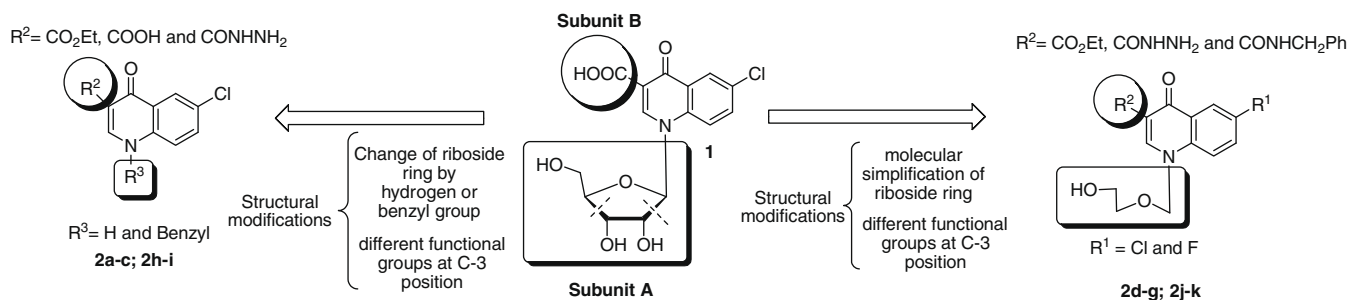
### 2.3. Molecular modeling analysis of oxoquinolines derivatives

Structure–activity relationship (SAR) studies of oxoquinolines revealed some important structural features apparently related to the anti-HIV activity. According to the theoretical results, the most active compounds (**2f**, **2g**, **2j**, and **2k**) with low toxicity risks in PBMC and high selective index showed low values of LUMO energy, which is related to a higher reactivity of the compound as electrophile. Most of the active compounds also presented higher number of hydrogen bond acceptor and donor groups as well as of rotatable bonds (Table 2) with lower dipole moment values (not shown). These features are also observed for compound **1** presenting the HIV-1 Reverse Transcriptase NNRTI binding pocket as target.<sup>13</sup>

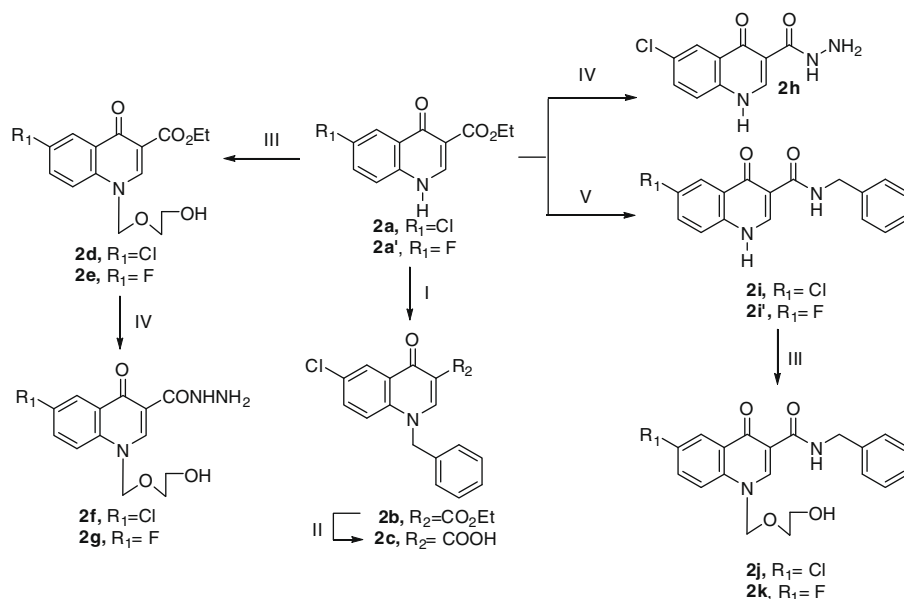
Since complementarity is essential for the interaction of active compounds with this target enzyme<sup>13</sup>, we analyzed the tridimensional structure and the electrostatic potential map, which allow the evaluation of size, shape, and superficial charge distribution to be related to the antiviral potency. Interestingly, in R<sup>3</sup>, compounds **2b–g**, **2j**, and **2k** present a similar overall shape with electronegative regions corresponding to the oxygen atom. The negative region in R<sup>2</sup> is related to the electron pair on nitrogen or the electron density on the phenyl ring (Fig. 1).

Since all active compounds present a substituent in the R<sup>3</sup> position, this structural feature seems to be important for their activity. The comparison of **2f** and **2j** with **2h** and **2i**, respectively, differing only in the R<sup>3</sup> position, clearly reinforced this hypothesis. The characteristic of the substituent is also important, since the active compounds present a hydrogen bond donor and a hydrogen bond acceptor in R<sup>3</sup>, in contrast to the less active compounds that present hydrophobic groups such as benzyl (**2b** and **2c**) (Fig. 1).

The comparison among compounds **2d**, **2f**, and **2j** as well as **2e**, **2g**, and **2k** showed that the hydrogen bond donor groups (nitrogen of amide or hydrazide) in the R<sup>2</sup> position may be an important



Scheme 1. Rational drug design for compounds **2a–k**.



**Scheme 2.** General synthetic route. Reagents and conditions: Route I—benzylchloride, DMF, K<sub>2</sub>CO<sub>3</sub>, 80 °C, 24 h; Route II—(a) NaOH/EtOH 1.0 M, rt, 3 h; (b) HCl 35 %; Route III—(a) BSTFA/TMSCl, CH<sub>3</sub>CN, reflux; (b) 1,3-dioxolane/TMSCl/KI, rt; (c) NaHCO<sub>3</sub>; Route IV—hydrazine monohydrate, 80%, EtOH, reflux, 1 h; Route V—benzylamine, phenyl ether, 210 °C, 1 h.

**Table 1**  
Anti-HIV-1 profile (% and EC<sub>50</sub>), cytotoxicity (CC<sub>50</sub>) and selective index (SI) of oxoquinoline derivatives **1** and **2a–k**

#	R <sup>1</sup>	R <sup>2</sup>	R <sup>3</sup>	HIV-1 inhibition (%)	EC <sub>50</sub> (μM)	CC <sub>50</sub> (μM)	SI
<b>1</b>	Cl	CO <sub>2</sub> H	β-D-Ribofuranosyl	99 ± 1.3	1.5 ± 0.2	1701 ± 10.1	1134
<b>2a</b>	Cl	CO <sub>2</sub> CH <sub>2</sub> CH <sub>3</sub>	H	58 ± 1.2	43.0 ± 1.2	1658 ± 9.8	39
<b>2b</b>	Cl	CO <sub>2</sub> CH <sub>2</sub> CH <sub>3</sub>	CH <sub>2</sub> Ph	24 ± 1.1	104.0 ± 4.5	1839 ± 12.2	18
<b>2c</b>	Cl	CO <sub>2</sub> H	CH <sub>2</sub> Ph	29 ± 2.0	86.0 ± 3.3	1890 ± 14.6	22
<b>2d</b>	Cl	CO <sub>2</sub> CH <sub>2</sub> CH <sub>3</sub>	CH <sub>2</sub> OCH <sub>2</sub> CH <sub>2</sub> OH	45 ± 3.3	50.0 ± 1.1	1800 ± 13.3	36
<b>2e</b>	F	CO <sub>2</sub> CH <sub>2</sub> CH <sub>3</sub>	CH <sub>2</sub> OCH <sub>2</sub> CH <sub>2</sub> OH	30 ± 1.4	83.3 ± 2.3	1500 ± 12.9	18
<b>2f</b>	Cl	CONHNH <sub>2</sub>	CH <sub>2</sub> OCH <sub>2</sub> CH <sub>2</sub> OH	99 ± 2.1	2.5 ± 4.4	2400 ± 10.5	960
<b>2g</b>	F	CONHNH <sub>2</sub>	CH <sub>2</sub> OCH <sub>2</sub> CH <sub>2</sub> OH	96 ± 1.3	3.3 ± 1.1	909 ± 9.1	275
<b>2h</b>	Cl	CONHNH <sub>2</sub>	H	29 ± 0.5	86.0 ± 2.8	1233 ± 12.5	14
<b>2i</b>	Cl	CONHCH <sub>2</sub> Ph	H	47 ± 0.7	53.0 ± 2.2	1395 ± 11.4	26
<b>2j</b>	Cl	CONHCH <sub>2</sub> Ph	CH <sub>2</sub> OCH <sub>2</sub> CH <sub>2</sub> OH	98 ± 0.9	4.5 ± 0.8	3200 ± 11.9	711
<b>2k</b>	F	CONHCH <sub>2</sub> Ph	CH <sub>2</sub> OCH <sub>2</sub> CH <sub>2</sub> OH	90 ± 1.0	2.8 ± 0.1	2800 ± 12.7	1000
<b>AZT</b>	—	—	—	94 ± 0.2	0.05 ± 0.002	126 ± 1.8	2520

**Table 2**  
Electronic properties and pharmacokinetic parameters important for good oral bioavailability of **2a–m**, AZT and efavirenz: HOMO energy (*E*<sub>HOMO</sub>), LUMO energy (*E*<sub>LUMO</sub>), number of hydrogen bond acceptor (*n*Hba), number of hydrogen bond donor (*n*Hbd), molecular weight (MW), calculated octanol/water partition coefficient (*cLog P*), number of rotatable bonds (*n*rotb) and the potential to qualify for a drug (druglikeness and drug-score)

#	Electronic properties		Lipinski 'rule of five'					Drug likeness	Drug score
	<i>E</i> <sub>HOMO</sub>	<i>E</i> <sub>LUMO</sub>	<i>n</i> HBA	<i>n</i> HBD	MW	<i>cLog P</i>	<i>n</i> rotb		
<b>1</b>	−8.40	1.61	8	4	355.73	0	7	0.27	0.7
<b>2a</b>	−8.78	1.74	4	1	251.67	1.85	3	−7.11	0.44
<b>2b</b>	−8.61	1.76	4	0	341.79	3.09	4	−5.15	0.34
<b>2c</b>	−8.68	1.70	4	1	313.74	2.20	4	2.90	0.60
<b>2d</b>	−8.92	1.62	6	1	325.75	1.02	7	−6.83	0.42
<b>2e</b>	−8.9	1.62	6	1	309.29	0.47	7	−8.64	0.26
<b>2f</b>	−8.92	1.46	7	4	311.72	−1.07	5	−2.83	0.36
<b>2g</b>	−8.98	1.46	7	4	295.27	−1.62	5	−4.64	0.27
<b>2h</b>	−8.68	1.57	5	4	237.65	−0.24	1	−2.85	0.38
<b>2i</b>	−8.76	1.64	4	2	312.76	2.31	2	4.07	0.76
<b>2j</b>	−8.82	1.53	6	2	386.83	1.48	7	4.31	0.71
<b>2k</b>	−8.83	1.52	6	2	370.38	0.93	7	2.56	0.45
<b>AZT</b>	—	—	9	2	267.25	−0.86	3	2.12	0.33
<b>Efavirenz</b>	—	—	3	1	315.68	4.24	1	−19.90	0.22

feature to interact with the target, since they are present in all of the most potent compounds, including **1**. The distribution of hydrogen bond donors and acceptors of the active derivatives is

similar to that of compound **1**, which reinforced the importance of this feature for the biological activity in contrast to the inactive derivatives, which only present hydrogen bond acceptors (Fig. 1).

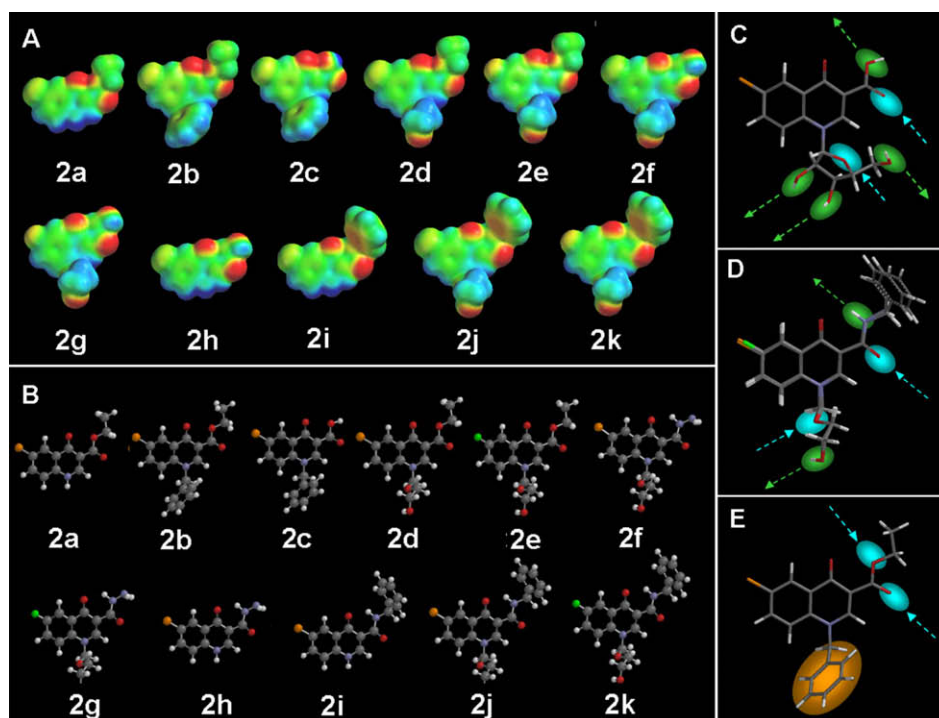


**Figure 1.** Structure of oxoquinoline derivatives. (A) Electrostatic potential map and (B) the most stable conformation of **2a–k**. (C) Structure of compound **1** that was used to design the oxoquinoline derivatives. (D) Structure alignment of the active compounds (**2f**, **2g**, **2j**, and **2k**) showing the pharmacophoric groups in the substituents. (E) Structure of the less active compounds (**2b**). Hydrophobic groups are shown in orange and hydrogen bond donors and acceptors in green and blue, respectively.

Interestingly, both halogen (chlorine and fluorine) groups could be used in these antiviral structures, since none of them compromised the activity (i.e., **2f**, **2g**, **2j**, and **2k**).

#### 2.4. In silico analysis of ADMET profile

The analysis of theoretical toxicity risks for the oxoquinoline derivatives using Osiris program showed compounds **2a**, **2d**, **2i**, and **2j** with low toxicity risks in contrast to AZT, the current antiviral used in HIV therapy, which presents reproductive and mutagenic effects (Fig. 2). Apparently, the mutagenic risk in **2e** and **2k** is associated to the fluoro substituent, since compounds **2d** and **2j**, which present the same substitutions, but chlorine instead of fluorine, showed no theoretical risks. Mutagenic risk also seems to be associated with the hydrazide group, since **2f**, **2g**, and **2h**, which present this group, are toxic in contrast to **2i** and **2j** (Fig. 2).

As these compounds are considered for oral delivery, they were submitted to the analysis of Lipinski 'rule of five'. This rule determines if a chemical compound presents absorption and permeation across membranes properties that would make it a likely orally active drug in humans. According to Lipinski, molecules

violating more than one of these rules may have problems with bioavailability.<sup>14</sup> Our results pointed that all compounds fulfill this rule and present molecular weight (237.65–386.83), cLog *P* (–1.62 to 3.09), *n*HBA (4–7), *n*HBD (0–4) and number of rotatable bonds (rotb) (1–7) similar to the commercial drugs AZT and efavirenz (Fig. 2).

Finally, we evaluated oxoquinoline derivatives **2a–k** as potential drugs by calculating druglikeness and drug-score. Druglikeness, which is related to the similarity with trade drugs (–9.42 to 4.31) was better than for the commercial drugs AZT (2.12) and efavirenz (–19.90). An analogous result was observed for the drug-score (0.13–0.76), (the current AZT = 0.33 and efavirenz = 0.22). Among the active compounds, **2j** showed the best values of druglikeness and drug-score (4.31 and 0.71, respectively) with a lower toxicity effect, which points it for further in vivo exploration (Table 2).

#### 3. Conclusion

In summary, a series of oxoquinoline derivatives with different substituents were synthesized and exhibited a significant anti-HIV

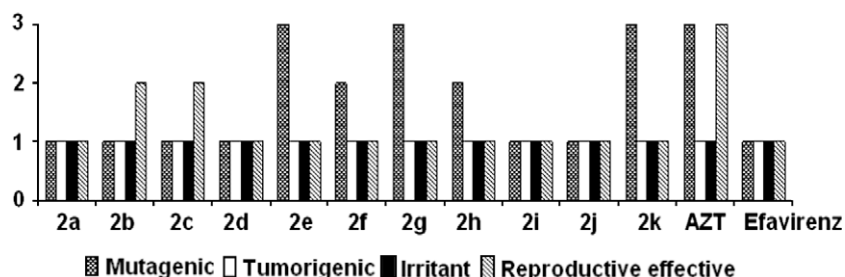


**Figure 2.** In silico toxicity risk analysis for oxoquinoline derivatives **2a–k** and commercial antivirals.



activity, suggesting their potential as antiviral agents. Molecular modeling analysis revealed stereoelectronic properties such as LUMO energy, dipole moment and number of rotatable bonds, hydrogen bond donors and acceptors as correlated with the compound potency. Based on this structural evaluation, a competitive mechanism of action is apparently not feasible, since these derivatives are not nucleoside analogs, but similar to compound **1**, which presents uncompetitive and noncompetitive modes of action against HIV1-reverse transcriptase.<sup>13</sup> Therefore, a further analysis to investigate these two feasible mechanisms of action should be considered.

Our studies pointed substituents in R<sup>2</sup> and R<sup>3</sup> as important for the biological activity, and compound **2j** as the best candidate for further investigation. This compound presents the best parameters including: (i) high activity against HIV-1, (ii) low cytotoxicity risks in PBMC, (iii) low toxic effect risks in *in silico* analysis, (iv) good oral bioavailability according to the Lipinski 'rule of five', and (v) better druglikeness and drug-score values than some commercial antivirals such as AZT and efavirenz (competitive and non competitive inhibitors, respectively). Overall, our results point to introducing structural changes at position 3 of the oxoquinoline ring of compound **2j** to increase its activity and verify the eventual effect at C-3 position. Thus, exploring the introduction of different electron-donating groups (i.e., -CH<sub>3</sub>, -NH<sub>2</sub>, and -OCH<sub>3</sub>) attached to the *N*-benzyl moiety of the carboxamide group may also enable the evaluation of not only electronic, but also steric parameters for improving the antiviral activity.

## 4. Experimental

### 4.1. Synthesis

#### 4.1.1. General procedures

Melting points were determined through a Fisher-Johns apparatus and are uncorrected. The IR spectra were recorded on a Perkin-Elmer FT-IR 1600 spectrometer as potassium bromide pellets and frequencies are expressed in cm<sup>-1</sup>. NMR spectra were recorded on a Varian Unity Plus 300 spectrometer operating at 300.13 MHz (<sup>1</sup>H) and 75.0 MHz (<sup>13</sup>C), in the specified solvents. Chemical shifts are reported in ppm ( $\delta$ ) relative to tetramethylsilane. Proton and carbon NMR spectra were typically obtained at room temperature. The two-dimensional experiments were acquired using standard Varian Associates automated programs for data acquisition and processing.

**4.1.1.1. Synthesis of 1-[(2'-hydroxyethoxy)methyl]-N-[(phenyl)methyl]-1,4-dihydro-4-oxoquinoline-3-carboxamides.** oxoquinolinecarboxamides (**2i** or **2i'**—3 mmol) were refluxed in bis(trimethylsilyl)trifluoroacetamide (BSTFA) (6.75 mmol) containing 1% TMSCL in 10 mL of acetonitrile, under nitrogen atmosphere, for 4 h, followed by addition of potassium iodide (3 mmol), 1,3-dioxolane (3 mmol), and TMSCL (3 mmol). The resulting mixture was stirred for 24 h at room temperature. Afterwards, it was poured into a mixture of ethyl alcohol/water (20 mL:10 mL), followed by addition of solid sodium bicarbonate (3 mmol) and subsequent stirring for 10 min, leading to the crude products, which were purified by crystallization from a mixture of ethyl alcohol/methylene chloride (1:1), giving the pure acyclonucleosides **2j** and **2k**. Compound **2j**: 6-chloro-1-[(2'-hydroxyethoxy)methyl]-N-[(phenyl)methyl]-1,4-dihydro-4-oxoquinoline-3-carboxamide (96% yield), mp 205–206 °C; IR (KBr) cm<sup>-1</sup> 3468, 1624, 1662; <sup>1</sup>H NMR (300.13 MHz, DMSO-*d*<sub>6</sub>, internal standard: Me<sub>4</sub>Si):  $\delta$  10.20 (t, *J* = 5.6 Hz, 1H, C=ONH); 9.80 (s, 1H, H-2); 8.23 (d, *J* = 2.4 Hz, 1H, H-5); 7.95 (d, *J* = 9.0 Hz, 1H, H-8); 7.89 (dd, *J* = 9.0; 2.4 Hz, 1H, H-7); 7.45 (m, 5H, H-3''–H-7''); 5.95 (s, 2H, H-1'); 4.65 (d, *J* = 5.6 Hz, 2H, H-1''); 3.52 (d, *J* = 5.4 Hz, 2H, H-3'); 3.46 (d,

*J* = 5.4 Hz, 2H, H-4'); <sup>13</sup>C NMR (75.0 MHz, DMSO-*d*<sub>6</sub>):  $\delta$  174.9 (C-4); 163.6 (C=ONH); 148.4 (C-2); 139.2 (C-2''); 137.5 (C-8a); 132.8 (C-7); 130.2 (C-6); 128.3 (C-5''); 128.0 (C-4a); 127.3 (C-3'' and C-7''); 126.8 (C-5); 124.7 (C-4'' and C-6''); 120.4 (C-8); 110.9 (C-3); 83.0 (C-1'); 70.1 (C-3'); 59.9 (C-4'); 42.2 (C-1''); HRMS (ESI) *m/z* calcd for C<sub>20</sub>H<sub>20</sub>ClN<sub>2</sub>O<sub>4</sub> [M+H]<sup>+</sup>: 387.1106, found 387.1111; **2k**: 6-fluoro-1-[(2'-hydroxyethoxy)methyl]-N-[(phenyl)methyl]-1,4-dihydro-4-oxoquinoline-3-carboxamide (83% yield), mp 159–161 °C; IR (KBr) cm<sup>-1</sup> 3498, 1602, 1655; <sup>1</sup>H NMR (300.13 MHz, DMSO-*d*<sub>6</sub>, internal standard: Me<sub>4</sub>Si):  $\delta$  9.06 (s, 1H, H-2); 8.16 (dd, *J* = 9.5; 4.4 Hz, 1H, H-5); 8.12 (dd, *J* = 9.0; 2.9 Hz, 1H, H-8); 7.72 (ddd, *J* = 9.0; 7.8; 2.9 Hz, 1H, H-7); 7.45 (m, 5H, H-3''–H-7''); 5.93 (s, 2H, H-1'); 4.73 (s, 2H, H-1''); 3.73–3.76 (m, 4H, H-3' and H-4'); <sup>13</sup>C NMR (75.0 MHz, DMSO-*d*<sub>6</sub>):  $\delta$  166.7 (C-4); 160.1 (C=ONH); 150.7 (C-3); 149.4 (C-2); 138.5 (d; <sup>1</sup>*J*<sub>C-F</sub> = 205.3; C-6); 137.2 (C-8a); 139.9 (C-2''); 129.7 (C-5''); 128.4 (C-4a); 128.5 (C-3'' and C-7''); 122.8 (d; <sup>2</sup>*J*<sub>C-F</sub> = 25.0 Hz; C-5); 128.4 (C-4' and C-6''); 122.1 (d; <sup>3</sup>*J*<sub>C-F</sub> = 8.3 Hz; C-8); 111.8 (d; <sup>2</sup>*J*<sub>C-F</sub> = 24.4 Hz; C-7); 85.5 (C-1'); 71.6 (C-3'); 61.9 (C-4'); 44.1 (C-1''); HRMS (ESI) *m/z* calcd for C<sub>20</sub>H<sub>20</sub>FN<sub>2</sub>O<sub>4</sub> [M+H]<sup>+</sup>: 371.1401 found 371.1407.

**4.1.1.2. Synthesis of 1-[(2'-hydroxyethoxy)methyl]-1,4-dihydro-4-oxoquinoline-3-carbohydrazides.** A solution of the appropriate acyclonucleosides (**2d** or **2e**—3.70 mmol) and 3.7 mL of 80% hydrazine monohydrate in 10 mL of ethanol, was stirred at reflux for 2 h. The reaction mixture was then concentrated under reduced pressure giving a colored solid which was collected by filtration, washed with cold ethyl acetate and dried under vacuum, leading to the desired hydrazides **2f** and **2g**. Compound **2f**: 6-chloro-1-[(2'-hydroxyethoxy)methyl]-1,4-dihydro-4-oxoquinoline-3-carbohydrazide (75% yield), mp 208–210 °C; IR (KBr) cm<sup>-1</sup> 3436, 3050, 1624, 1650; <sup>1</sup>H NMR (300.13 MHz, DMSO-*d*<sub>6</sub>, internal standard: Me<sub>4</sub>Si):  $\delta$  10.45 (sl, 1H, C=ONHNH<sub>2</sub>); (8.97 (s, 1H, H-2); 8.25 (d, *J* = 2.4 Hz, 1H, H-5); 7.95 (d, *J* = 9.0 Hz, 1H, H-8); 7.89 (dd, *J* = 9.0; 2.4 Hz, 1H, H-7); 5.86 (s, 2H, H-1'); 3.50–3.55 (m, 4H, H-3' and H-4'); 3.39 (sl, 2H, C=ONHNH<sub>2</sub>); <sup>13</sup>C NMR (75.0 MHz, DMSO-*d*<sub>6</sub>):  $\delta$  176.1 (C-4); 164.8 (C=ONHNH<sub>2</sub>); 139.0 (C-6); 149.5 (C-2); 129.5 (C-4a); 134.4 (C-8); 131.9 (C-8a); 126.4 (C-5); 122.0 (C-7); 112.1 (C-3); 84.5 (C-1'); 71.6 (C-3'); 61.4 (C-4') HRMS (ESI) *m/z* calcd for C<sub>13</sub>H<sub>15</sub>ClN<sub>3</sub>O<sub>4</sub> [M+H]<sup>+</sup>: 312.0745 found 312.0751; **2g**: 6-fluoro-1-[(2'-hydroxyethoxy)methyl]-1,4-dihydro-4-oxoquinoline-3-carbohydrazide (70% yield), mp 202–203 °C; IR (KBr) cm<sup>-1</sup> 3399, 3048, 1606, 1650; <sup>1</sup>H NMR (300.13 MHz, DMSO-*d*<sub>6</sub>, internal standard: Me<sub>4</sub>Si):  $\delta$  8.99 (s, 1H, H-2); 8.24 (dd, *J* = 7.0; 2.3 Hz, 1H, H-5); 7.95 (dd, *J* = 9.1; 7.0 Hz, 1H, H-8); 7.88 (ddd, *J* = 9.1; 7.0; 2.3 Hz, 1H, H-7); 5.69 (s, 2H, H-1'); 4.61 (t, *J* = 5.0 Hz, 2H, C=ONHNH<sub>2</sub>); 3.52 (dd, *J* = 9.4; 5.3 Hz, 2H, H-3'); 3.47 (dd, *J* = 9.4; 5.3 Hz, H-4'); <sup>13</sup>C NMR (75.0 MHz, DMSO-*d*<sub>6</sub>):  $\delta$  174.8 (C-4); 165.2 (C=ONHNH<sub>2</sub>); 159.4 (d; <sup>1</sup>*J*<sub>C-F</sub> = 245.2 Hz; C-6); 147.6 (C-2); 128.4 (d; <sup>3</sup>*J*<sub>C-F</sub> = 7.1 Hz; C-4a); 121.1 (d; <sup>3</sup>*J*<sub>C-F</sub> = 8.3 Hz; C-8); 135.4 (d; <sup>4</sup>*J*<sub>C-F</sub> = 1.2 Hz; C-8a); 121.4 (d; <sup>2</sup>*J*<sub>C-F</sub> = 25.0 Hz; C-5); 110.2 (d; <sup>2</sup>*J*<sub>C-F</sub> = 22.6 Hz; C-7); 110.5 (C-3); 83.0 (C-1'); 70.0 (C-3'); 59.9 (C-4'); HRMS (ESI) *m/z* calcd for C<sub>13</sub>H<sub>15</sub>FN<sub>3</sub>O<sub>4</sub> [M+H]<sup>+</sup>: 296.1041 found 296.1046.

### 4.2. Biological evaluation

#### 4.2.1. Cells and virus

Peripheral blood mononuclear cells (PBMCs) from healthy human donors were obtained by density gradient centrifugation (Hystopaque, Sigma) from buffy coat preparations. PBMCs were resuspended in RPMI 1640 (LGC Bio, São Paulo, SP, Brazil) supplemented with 10% heat-inactivated fetal bovine serum (FBS, Hyclone, Logan, UT), penicillin (100 U/mL), streptomycin (100 µg/mL), 2 mM glutamine and 10 mM HEPES, stimulated with 5 µg/mL of phytohemagglutinin (PHA, Sigma) for two to three days, and further maintained in culture medium containing 5 U/mL of

recombinant human interleukin-2 (Sigma). The virus isolate Ba-L (R5-tropic, subtype B<sup>15</sup>) was used for cell infections, and virus stocks were prepared in PHA-activated PBMCs from normal donors.

#### 4.2.2. Evaluation of cytotoxic effects

**4.2.2.1. Cytotoxicity in peripheral blood mononuclear cells (PBMCs).** The cytotoxic effect was determined colorimetrically using XTT method.<sup>16</sup> In brief, 50  $\mu$ L of XTT were added to cells and the optical density was measured at 450 nm 2 h later. The 50% cytotoxic concentration (CC<sub>50</sub>) was defined as the concentration ( $\mu$ M) that reduced cell viability by 50% when compared to untreated controls.

**4.2.2.2. Cytotoxicity in *vero* cells.** Vero cells were cultured in Dulbecco's modified Eagle's medium (DMEM) supplemented with 5% fetal bovine serum (FBS; HyClone, Logan, Utah), 100 U/mL penicillin and 100  $\mu$ g/mL streptomycin, at 37 °C in 5% CO<sub>2</sub>.

Monolayer of 10<sup>4</sup> vero cells in 96-multiwell plates was treated with various concentrations of the compounds for 72 h. Then, 50  $\mu$ L of 1 mg/mL solution of 3-(4,5-dimethylthiazol-2-yl)-2,5-diphenyl tetrazolium bromide (MTT; Sigma) was added to evaluate cell viability according to procedures described elsewhere.<sup>17</sup> The 50% cytotoxic concentration (CC<sub>50</sub>) was calculated by linear regression analysis of the dose–response curves.

#### 4.2.3. Anti-hiv-1 activity

The effect on HIV replication was analyzed using PBMC initially exposed to viral suspensions containing 5–10 ng/mL of HIV-1 p24Ag for 2–3 h. Cells were washed, resuspended in complete medium, plated in 96-well culture plates (2  $\times$  10<sup>5</sup> cells/well) in triplicates, and treated with different concentrations of the compounds. After 7 days at 37 °C in 5% CO<sub>2</sub>, viral replication was assessed by measuring the HIV-1 p24Ag in culture supernatants by ELISA capture assay (ZeptoMetrix Co., Buffalo, NY). Viral replication was evaluated by measuring the HIV-1 p24Ag in culture supernatants.

#### 4.3. Molecular modeling, SAR studies and in silico ADMET screening

Initially, the structures were submitted to a conformational analysis procedure available in the SPARTAN'06 software package (Wavefunction Inc. Irvine, CA, 2000), using the MMFF94 force field. The most stable conformers were submitted to a full geometry optimization process, using the AM1 semiempirical Hamiltonian, and, subsequently, to a single-point energy *ab initio* calculation, at the 6–311G<sup>+</sup> level, both methods available in SPARTAN'06. The stereoelectronic properties of all structures were evaluated in order to perform structure–activity relationship (SAR) studies. Values of HOMO (Highest Occupied Molecular Orbital) and LUMO (Lowest Unoccupied Molecular Orbital) energy, molecular weight, volume, and surface area, HOMO and LUMO orbital coefficients distribution, molecular dipole moment ( $\mu$ ), and molecular electrostatic potential (MEP) maps were calculated. MEP isoenergy surface maps were generated in the range of –150.0 (deepest red color) to +150.0 (deepest blue color) kJ/mol and superimposed onto a molecular surface of constant electron density of 0.002 e/au<sup>3</sup>.<sup>12</sup>

In addition, descriptors such as cLog *P* (octanol/water partition coefficient) and Log *S* (water solubility) were calculated using the Osiris Property Explorer on-line system available at <http://www.organic-chemistry.org/prog/peo/>.

The oxoquinoline derivatives were submitted to in silico ADMET (absorption, distribution, metabolism, excretion, and toxicity) screening, using the Osiris program. Values of druglikeness are based on the occurrence frequency of each fragment of the molecule in commercial drugs while the drug-score evaluates the com-

pound's potential to qualify for a drug and is related to topological descriptors, fingerprints of molecular druglikeness, structural keys and other properties such as cLog *P* and molecular mass.<sup>18</sup>

The pharmacokinetic profile, important for a good oral bioavailability of a compound, was also evaluated according to the Lipinski's 'rule-of-five', which analyses features that a drug should present to allow the absorption and permeation across the membranes and states molecular weight  $\leq$ 500 daltons (Da), calculated octanol/water partition coefficient (cLog *P*)  $\leq$ 5, number of hydrogen-bond acceptors (nHba)  $\leq$ 10, and number of hydrogen-bond donors (nHbd)  $\leq$ 5 (Lipinski, 2001), as well as a fifth rule added later, which infers the number of rotatable bonds  $\leq$ 10.<sup>19</sup>

#### Acknowledgments

We thank the Conselho Nacional de Desenvolvimento Científico e Tecnológico (CNPq), Coordenação de Aperfeiçoamento de Pessoal Docente (CAPES) and Fundação de Amparo à Pesquisa do Estado do Rio de Janeiro (FAPERJ) for the financial support. Thanks are also due to HU/UFRJ hemotherapy service and NIH AIDS Reagent Program. The technical assistance of Samara and Hania is gratefully acknowledged. The authors also thank Professor Gilberto Alves Romeiro (UFF) and Professor Marcos Eberlin (UNICAMP) for recording the HRMS spectra.

#### References and notes

- (a) Snyder, S.; D'Argenio, D. Z.; Weislow, O.; Bilello, J. A.; Drusano, G. L. *Antimicrob. Agents Chemother.* **2000**, *44*, 1051; (b) Stebbing, J.; Bower, M.; Mandalia, S.; Nelson, M.; Gazzard, B. *Clin. Exp. Immunol.* **2006**, *1452*, 271.
- Stevenson, M. *Sci. Am.* **2008**, 299, 78.
- (a) Zhang, Z.; Fu, J.; Zhao, Q.; He, Y.; Jin, L.; Zhang, H.; Yao, J.; Zhang, L.; Wang, F. *J. Immunol.* **2006**, *176*, 5644; (b) Rodriguez-Arenas, M. A.; Jarrin, I.; Del Amo, J.; Iribarren, J. A.; Moreno, S.; Viciano, P.; Pena, A.; Gomez Sirvent, J. L.; Vidal, F.; Lacruz, J.; Gutierrez, F.; Oteo, J. A.; Asencio, R.; Castilla, J.; Perez Hoyos, S. *AIDS Res. Hum. Retroviruses* **2006**, *22*, 715; (c) Sabin, C. A.; Smith, C. J.; Youle, M.; Lampe, F. C.; Bell, D. R.; Puradiredja, D.; Lipman, M. C. I.; Bhagani, S.; Phillips, A. N.; Johnson, M. A. *AIDS* **2006**, *20*, 67.
- (a) Baba, M.; Okamoto, M.; Makino, M.; Kimura, Y.; Ikeuchi, T.; Sakaguchi, T.; Okamoto, T. *Antimicrob. Agents Chemother.* **1997**, *41*, 1250; (b) Cecchetti, V.; Parolin, C.; Moro, S.; Pecere, T.; Filippini, E.; Calistri, A.; Tabarrini, O.; Gatto, B.; Palumbo, M.; Fravolini, A.; Palu, G. *J. Med. Chem.* **2000**, *43*, 3799.
- (a) Canuto, C. V. B. S.; Gomes, C. R. B.; Marques, I. P.; Faro, L. V.; Santos, F. C.; Frugulhetti, I. C. P. P.; Souza, T. M. L.; Cunha, A. C.; Romeiro, G. A.; Ferreira, V. F.; Souza, M. C. B. V. *Lett. Drug Des. Discovery* **2007**, *4*, 404; (b) Souza, T. M. L.; Cirne-Santos, C. C.; Rodrigues, D. Q.; Abreu, C. M.; Tanuri, A.; Ferreira, V. F.; Marques, I. P.; Souza, M. C. B. V.; Fontes, C. F. L.; Frugulhetti, I. C. P. P.; Bou-Habib, D. C. *Curr. HIV Res.* **2008**, *6*, 209.
- Souza, T. M.; Souza, M. C. B. V.; Ferreira, V. F.; Canuto, C. V.; Marques, I. P.; Fontes, C. F.; Frugulhetti, I. C. P. P. *Arch. Virol.* **2007**, *152*, 1417.
- (a) Deffin, G. F.; Kendall, J. D. *J. Am. Chem. Soc.* **1948**, *70*, 893; (b) Snyder, H. R.; Freier, H. E.; Kovacic, P.; Heyningen, E. M. V. *J. Am. Chem. Soc.* **1947**, *69*, 371.
- Tsuchiya, S.; Hiratsuka, K.; Yasuda, N.; Fukuzaki, A. *Worldwide Patent*, WO 92,21,658, 1992, 92 pp.
- He, J. F.; Yun, L. H.; Yang, R. F.; Xiao, Z. Y.; Cheng, J. P.; Zhou, W. X.; Zhang, Y. X. *Bioorg. Med. Chem. Lett.* **2005**, *15*, 2980.
- (a) Al-Soud, Y. A.; Al-Masoudi, N. A. *J. Braz. Chem. Soc.* **2003**, *14*, 790; (b) Cunha, A. C.; Figueiredo, J. M.; Tributino, J. L. M.; Miranda, A. L. P.; Castro, H. C.; Zingali, R. B.; Fraga, C. A. M.; Souza, M. C. B. V.; Ferreira, V. F.; Barreiro, E. J. *Bioorg. Med. Chem.* **2003**, *11*, 2051.
- Lucero, B. A.; Gomes, C. R. B.; Frugulhetti, I. C. P. P.; Faro, L. V.; Alvarenga, L.; Souza, M. C. B. V.; Souza, T. M. L.; Ferreira, V. F. *Bioorg. Med. Chem. Lett.* **2006**, *16*, 1010.
- Silva, F. C.; Souza, M. C. B. V.; Frugulhetti, I. C. P. P.; Castro, H. C.; Souza, S. L. O.; Souza, T. M. L.; Rodrigues, D. Q.; Souza, A. M. T.; Abreu, P. A.; Passamani, F.; Rodrigues, C. R. *Eur. J. Med. Chem.* **2009**, *44*, 373.
- Souza, T. M. L.; Rodrigues, D. Q.; Ferreira, V. F.; Marques, I. P.; Santos, F. C.; Cunha, A. C.; Souza, M. C. B. V.; Frugulhetti, I. C. P. P.; Bou-Habib, D. C.; Fontes, C. F. L. *Curr. HIV Res.* **2009**, *7*, 327.
- Lipinski, A. C.; Lombardo, F.; Dominy, B. W.; Feeney, P. J. *Adv. Drug Delivery Rev.* **1997**, *23*, 3.
- Lima, R. G.; Van, W. J.; Saraiva, E. M. B.; Barral-Netto, M.; Galvao-Castro, B.; Bou-Habib, D. C. *J. Infect. Dis.* **2002**, *185*, 1561.
- Scudiero, D. A.; Shoemaker, R. H.; Paull, K. D.; Monks, A.; Tierney, S.; Nofziger, T. H.; Currens, M. J.; Seniff, D.; Boyd, M. R. *Cancer Res.* **1988**, *48*, 4827.
- Mosmann, T. *J. Immunol. Methods* **1983**, *65*, 55.
- Tekto, I. V. *Drug Discovery Today* **2005**, *10*, 1497.
- Wenlock, M. C.; Austin, R. P.; Barton, P.; Davis, A. M.; Leeson, P. D. *J. Med. Chem.* **2003**, *46*, 1250.